



HAL
open science

Anisotropic cellular forces support mechanical integrity of the Stratum Corneum barrier

Shuo Guo, Yegor Domanov, Mark Donovan, Bertrand Ducos, Yves Pomeau, Christine Gourier, Eric Perez, Gustavo S. Luengo

► **To cite this version:**

Shuo Guo, Yegor Domanov, Mark Donovan, Bertrand Ducos, Yves Pomeau, et al.. Anisotropic cellular forces support mechanical integrity of the Stratum Corneum barrier. *Journal of the mechanical behavior of biomedical materials*, 2019, 92, pp.11-23. 10.1016/j.jmbbm.2018.12.027 . hal-01991316

HAL Id: hal-01991316

<https://hal.sorbonne-universite.fr/hal-01991316v1>

Submitted on 25 Jan 2019

HAL is a multi-disciplinary open access archive for the deposit and dissemination of scientific research documents, whether they are published or not. The documents may come from teaching and research institutions in France or abroad, or from public or private research centers.

L'archive ouverte pluridisciplinaire **HAL**, est destinée au dépôt et à la diffusion de documents scientifiques de niveau recherche, publiés ou non, émanant des établissements d'enseignement et de recherche français ou étrangers, des laboratoires publics ou privés.

Anisotropic cellular forces support mechanical integrity of the Stratum Corneum barrier

Shuo Guo^a, Yegor Domanov^b, Mark Donovan^b, Bertrand Ducos^a, Yves Pomeau^c, Christine
Gourier^a, Eric Perez^{a,*}, and Gustavo S. Luengo^{b,*}

^a *Laboratoire de Physique Statistique, Ecole Normale Supérieure, l'université de recherche Paris
Sciences et Lettres, CNRS UMR 8550, Sorbonne Universités, Université Pierre-et-Marie-Curie (UPMC)
University of Paris 06, Université Paris Diderot, 75005 Paris, France*

^b *L'Oréal Research and Innovation, 93600 Aulnay-sous-bois, France*

^c *University of Arizona, Department of Mathematics, Tucson, AZ, USA*

(*) To whom correspondence should be addressed. Eric Perez E-mail: perez@lps.ens.fr and Gustavo S. Luengo
gluengo@rd.loreal.com

ABSTRACT

The protective function of biological surfaces that are exposed to the exterior of living organisms is the result of a complex arrangement and interaction of cellular components. This is the case for the most external cornified layer of skin, the stratum corneum (SC). This layer is made of corneocytes, the elementary 'flat bricks' that are held together through adhesive junctions. Despite the well-known protective role of the SC under high mechanical stresses and rapid cell turnover, the subtleties regarding the adhesion and mechanical interaction among the individual corneocytes are still poorly known. Here, we explore the adhesion of single corneocytes at different depths of the SC, by pulling them using glass microcantilevers, and measuring their detachment forces. We measured their interplanar adhesion between SC layers, and their peripheral adhesion among cells within a SC layer. Both adhesions increased considerably with depth. At the SC surface, with respect to adhesion, the corneocyte population exhibited a strong heterogeneity, where detachment forces differed by more than one order of magnitude for corneocytes located side by side. The measured detachment forces indicated that in the upper-middle layers of SC, the peripheral adhesion was stronger than the interplanar one. We conclude that the stronger peripheral adhesion of corneocytes in the SC favors an efficient barrier which would be able to resist strong stresses.

Keywords

Skin barrier, cell adhesion, stratum corneum, corneocyte, adhesion

1. Introduction

The variety of structures and shapes found on biological surfaces of living organisms exposed to the external environment is remarkable. Nature chooses particular arrangements of cellular components to maintain mechanical consistency, resistance to wear and in general to protect the organism (1). This variety is the result of subtle transformation and reorganization of a tissue's constitutive cells to create a complex network of cell-cell interactions that scaffolds the structure while providing one of its main functions, protection from the external environment.

Human skin is a good example (2). It is the largest organ of the body, which protects and helps regulate its temperature. In particular, its most external part, the stratum corneum (SC), is the main barrier that protects us from the external environment insults such as chemicals and microbes, and strictly limits transepidermal water loss (3). The SC is a multilayered tissue composed of alternating layers of lipids and cornified cells called corneocytes. The latter are terminally differentiated cells which are relatively flat, 0.1 – 0.5 μm thick, with a polygonal shape and with a lateral size of 30-50 μm . A corneocyte is surrounded by a highly cross-linked protein envelope and adheres to its neighboring cells through junctions known as corneodesmosomes (4,5).

Corneocytes are shed progressively from the surface of the SC through a process known as desquamation. This is an enzymatic process which involves the degradation of the key glycosylated protein components of corneodesmosomes, notably desmoglein 1 and corneodesmosin, and by the serine protease kallikrein 7 (6). The spatial distribution of corneodesmosomes and the major corneodesmosomal proteins, desmoglein 1 and corneodesmosin, have been mapped on the surface of corneocytes throughout the SC using electron microscopy, immunohistochemical and atomic force microscopic (AFM) approaches (7-12). In particular, AFM studies with a functionalized tip mapped accurately corneodesmosomes on the surface of SC, but also in the inner layers (7). These inner layers were made accessible by performing tape-stripping. They were found to display corneodesmosomes, showing that the detachment by tape-stripping takes place between the corneocytes. Morphological changes in desmosomes and corneodesmosomes and partial detachment of corneocytes prior to desquamation were monitored by Transmission Electron microscopy (TEM) (13). The surface density of corneodesmosomes is greater on corneocytes present in the lower levels of the SC with a relatively even distribution across the lateral surface of the corneocyte and at the periphery. In the upper layers of the SC, corneodesmosomes are mostly found at the periphery of the corneocyte surface with a considerably reduced presence on lateral surfaces.

It is truly remarkable that the SC is able to play its essential protective barrier function in the context of its fast cell turnover, which is completed within 3 weeks, and dramatic mechanical stresses experienced by the skin surface, such as bending, stretching, rubbing and scratching. This role is closely related to the minutely controlled elastic and adhesive properties of the corneocytes, which we explored in the present study.

Macroscopic evidence indicates that the strength of corneocyte adhesion increases with depth in the SC (14,15). Tape-stripping is often used to study SC at different depths

(15,16,17), and the separation is known to take place at the weakest corneocyte interface (14). Consecutive tape-stripping has shown that the adhesion of the outer layers of SC is weaker than the adhesion of the inner layers. Wu et al. (14), for example, determined delamination energies (4-60 J/m²) which depended on the delamination order, from mechanical macroscopic experiments in air. Measurements of the mechanical properties of individual corneocytes have been reported as well. Using two glass needles, Lévêque and coworkers (18) have measured the Young's modulus of single corneocytes in aqueous medium (0.45 GPa) and the force needed (0 to 190 μN) to separate two adhering corneocytes. In spite of this knowledge, information on single corneocyte adhesion with its neighboring cells in ambient air conditions, which is the biologically relevant condition, is still lacking.

This paper explores the adhesion of single corneocytes in different layers of the SC by using glass micro-cantilevers as force probes. When glued to the SC, these micro-cantilevers were maneuvered to pull corneocytes off the SC and detachment forces were measured. The corneocytes were in their native state as they were detached mechanically from SC in air without the action of chemicals or excess water. This technique distinguishes the interplanar adhesion of corneocytes from their peripheral adhesion, i.e. the one that occurs between their edges. Both types of adhesion were shown to increase in the deeper layers of SC and a clear difference between interplanar and peripheral adhesions was observed in the outer layers. As the exposition to different relative humidity (RH) levels can affect the efficiency of the stratum corneum barrier (3) through the ensuing modification of the adhesive strength of the corneocytes, the effect of RH on the adhesion of corneocytes is also presented.

2. Materials and methods

2.1 Stratum Corneum samples:

Human abdominal skin residues from plastic surgery were supplied in frozen form. They were obtained according to the ethical principles stated in the Helsinki declaration. SC was isolated using a standard protocol (19). Subcutaneous fat was removed and the dermis was separated from epidermis by immersing skin into hot water (56°C). Remaining viable epidermis was removed by tryptic digestion at 37°C overnight. The SC was dried and stored at room temperature (T=21°C) and ambient humidity (relative humidity (RH) of 45%). In this study, the SC from three healthy Caucasian female donors (aged 29, 36 and 41) was used.

2.2 Glass microcantilevers for force measurements:

Glass rods (Harvard Apparatus, 30-0086) were stretched and bent, using a pipette puller (Sutton Sutter P-2000) and a home-made micro-forge, to form micro-cantilevers with a diameter of ~10 μm, a length of ~5 mm and a height of ~50 μm (Figs. 1-2). The cantilevers were calibrated against a known pushing force produced by another calibrated cantilever. The stiffnesses of the cantilevers that were used ranged from 8 to 30 N/m, producing an error bar of ±3 to ±10 μN. All the force measurements were performed in air.

2.3 Measurement of the detachment force of one corneocyte from the SC:

One cantilever was fixed to a 3-axis micromanipulator (Narishige, Japan) by means of a pipette holder (Narishige, Japan). A 1mmx2mm piece of SC was glued (the inner/epidermal side of SC always facing the glass support) on a thick rigid glass rod (1mm diameter) that was fixed to a second micromanipulator. The setup was placed on the stage of an inverted microscope (Leica DMIRB) and the observations were made with x63 and x20 air objectives. The whole microscope and micromanipulators were enclosed in a Perspex box in which the relative humidity (RH) of the air was controlled. Each SC sample was equilibrated for 6 hours at the constant RH used prior to measurements that were performed at 25%, 44%, and 71% RH.

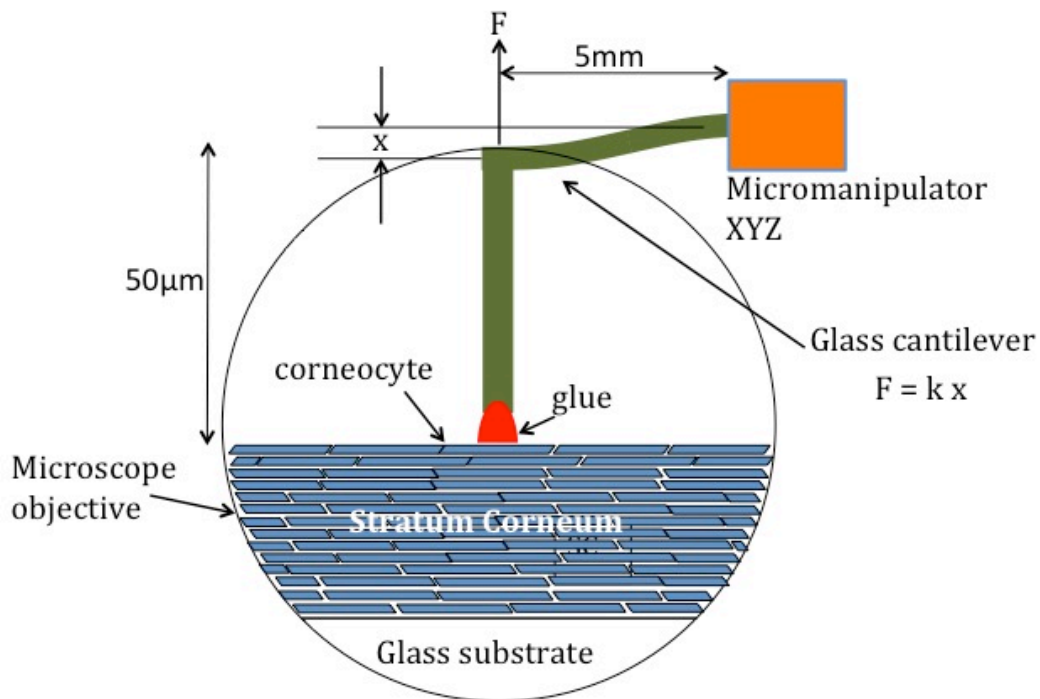


Fig. 1: Principle of detachment force measurements. Schematics (not to scale) of micro-cantilever with a stiffness k glued to the stratum corneum (SC) as seen through the microscope objective. The surface of the SC is perpendicular to the focal plane of the microscope and parallel to the optical axis, so that in the field of view, the gluing and the corneocyte detachment can be monitored. To measure the detachment force, the cantilever holder is moved away until the corneocyte detaches at a given bending of the cantilever that determines the force.

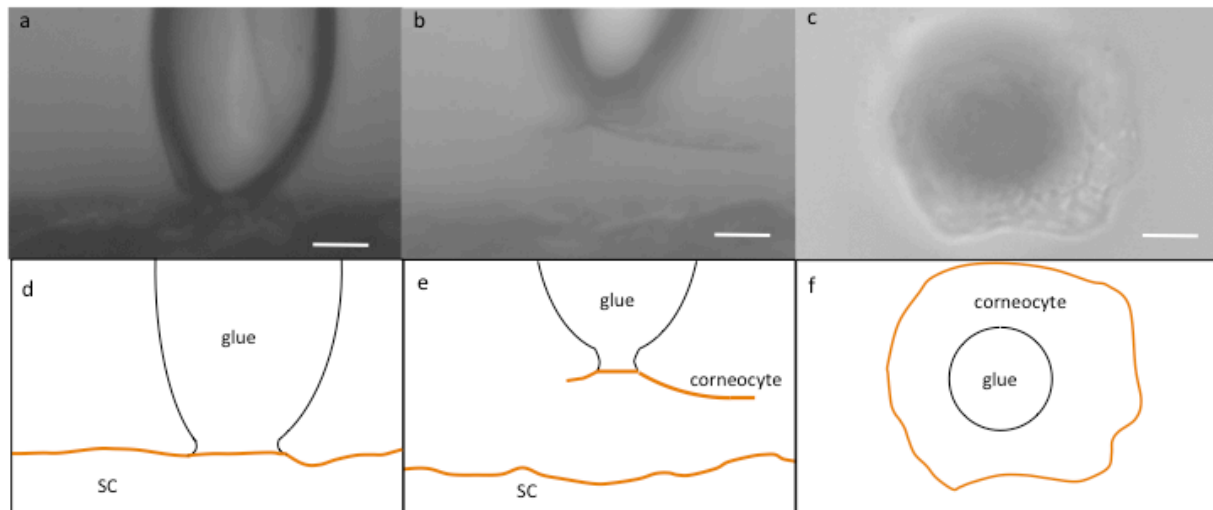


Fig. 2: Microscopic view of the stratum corneum (SC), the corneocyte and the glue. (a) Glue drop in contact with SC (the cantilever is above the glue – not shown-); (b) a corneocyte detached from SC after pulling; (c) a corneocyte observed after 90° rotation of cantilever. The darker zone is the glue/corneocytes interface. The scale bar is 10 μ m. Bottom d, e, f: sketches that allow to see the shape of the glue, corneocyte and SC.

UV-setting glue (Loctite 3526) was used to adhere the tip of the cantilever to one region of SC and pull on it. With the SC surface parallel to the optical axis and the cantilever in the focal plane of the microscope, it was possible to glue the cantilever tip and to follow its detachment from the SC. However, the quality of the images was low and it did not allow to localize the corneocytes' borders, and therefore the position of the cantilever on the SC surface was randomly chosen. The glue was irradiated during 2 minutes (SpotCure-B lamp, wavelength: 365nm; power: 1 Watt/cm²) with UV light for curing. Then the cantilever was slowly moved away from the SC with the micromanipulator (operated manually but regularly at a few μ m per second) by a known distance until it detached from the SC. The force applied by the cantilever in order to detach corneocytes was generated by displacing the cantilever holder. The speed of the displacement, when multiplied by the cantilever stiffness is equal to the rate of increase of the force (the load) which increases until detachment. The loading rate (LR) is the rate at which the pulling force increases and it is expressed in μ N/s. As the micromanipulator was operated manually, the loading rate was not controlled but it was measured. The bending of the cantilever was equal to the difference between its displacement and the stretching of the SC under the tension imposed by the cantilever. The separation force was equal to the cantilever bending multiplied by the stiffness of the cantilever at the time of the detachment. Once the measurement was done, the cantilever was moved sideways by 200 μ m and new measurements were done, repeatedly every 200 μ m.

It may be possible that some penetration of the glue takes place between corneocytes. Had this been the case, 3-D aggregates of corneocytes would be detached and this would have required a stronger force to do so. In the pulling experiments, the strong forces have been only observed when the glue leaves the SC without detaching a corneocyte. Moreover, as the number of corneodesmosome linkages per corneocyte are known to decrease as one moves towards the SC surface (13), one would expect less penetration

of the glue in the deeper layers, and therefore smaller detachment forces of the glue. This was not observed, and thus it can be concluded that the glue does not penetrate into the SC during the pulling experiments.

After detaching the cantilever from the SC and measuring the separation force, the cantilever was rotated by 90 degrees in order to observe, with the microscope, what was left at the glue surface (Fig. 1-2 and video:

<https://drive.google.com/file/d/1qdfwxguJ9cHrtjo12POq39yN-djNACl/view?usp=sharing>).

This determined (i) whether none, one, or some of the corneocytes were detached, and (ii) whether the position of the cantilever was close to the center of one corneocyte, or over two corneocytes. When no corneocyte was detached from the SC, the measured force was F_{g-c} , the force needed to separate the glue from the SC. The glue diameter was chosen to be between 10 and 20 μm which was lower than the size (30-50 μm) of a corneocyte.

The corneocytes from the deeper layers of SC were explored by the scotch tape-stripping method (16,17). This involved adhering a scotch-tape to the SC and then detaching it; this removes approximately one corneocyte layer. This procedure was repeated several times until the appropriate depth level was reached. Thus 0, 4 and 9 consecutive strips were performed for sampling the 1st, 5th and 10th layers of the SC that were the ones referred to in this article. It may happen that more than one corneocyte layer is removed by tape-stripping. This study does not pretend to be absolutely accurate about the depth at which the measurements were done. However, it can be stated that three different levels of SC were studied:

- at the surface, when no tape strip is done, is the stratum disjunctum, and is referred to as the 1st layer
- after 4 tape strips, one is located below the stratum disjunctum, and this is referred to as the 5th layer
- after 9 tape strips, one is located in the middle of stratum compactum, and this is referred to as the 10th layer.

The reference to the 1st, 5th and 10th layers is only approximate and these refer to the stratum disjunctum, below the stratum disjunctum, and the middle of stratum compactum respectively.

2.4 Laser micro-dissection experiments

To further probe the adhesion of corneocytes, Laser Micro-dissection (LMD) was performed on SC prior to pulling, in order to remove the links of corneocytes with their neighbors of the same layer. This technique made a superficial cut on a chosen contour on SC. This was performed by a Leica LMD7000 unit. A superficial dissection was made along circles of 30-40 μm diameter (Power: 120 μJ /pulse, pulse frequency: 10Hz, Fig. 3a). The parameters were chosen in such a way that the cut would be as superficial as possible. The depth of the cut can be estimated from the microscope view of the profile of SC after LMD (video at:

https://drive.google.com/file/d/1xplHXutfY5Z_8x7XwUOnYUEaao5yxSBD/view?usp=sharing), and it is about 2.5-3 μm . Then, the cantilever was glued at the center of the circle (Fig. 3b) and the detachment experiment was performed as described above.

As the LMD achieves the cutting by focusing a UV laser onto the SC surface, it is necessary to check whether the LMD overheats the SC and destroys the

corneodesmosomes at some distance from the cut, reducing artificially the corneocytes' adhesion. Controls of LMD experiments were made by performing detachment experiments outside these circles at a distance of 10 μ m from them (Fig. 3c). They were done by gluing the cantilever tip close (at 10 μ m) but outside the circles along which the LMD was performed.

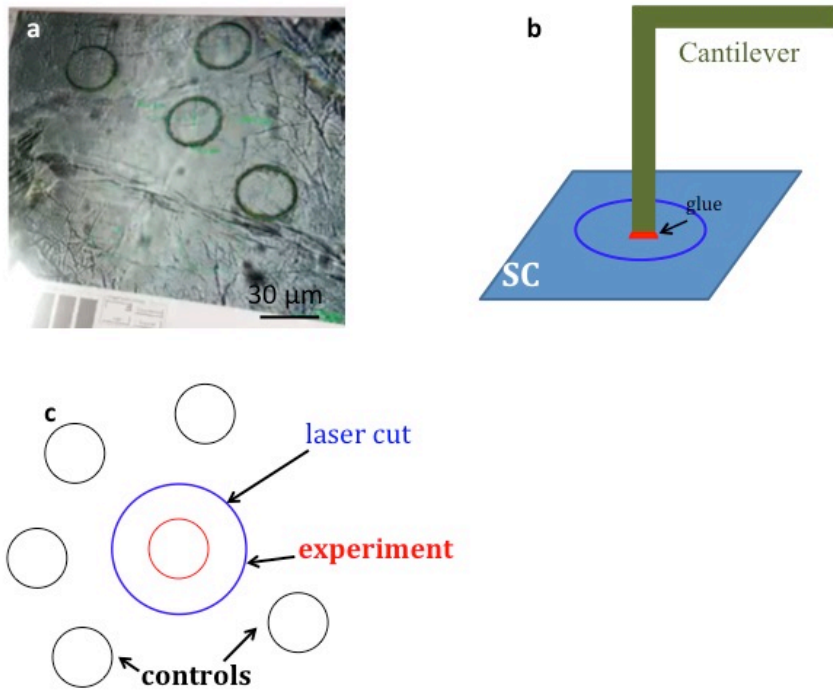


Fig. 3: Laser micro-dissection experiments. (a) Photo of the stratum corneum after laser micro-dissection; the dark lines are where the micro-dissection has been made; (b) and (c) configuration of the pulling experiments after LMD with the glue indicated by a red circle, and configuration of the controls with the glue indicated by black circles.

2.4 Measurement of the detachment force of two corneocytes adhering by their edges:

To perform this measurement, pre-formed doublets of corneocytes adhering by their edges were used. These doublets were available when a doublet was detached in a pulling experiment, instead of a single corneocyte. One of the corneocytes of the doublet was glued to one cantilever and the other one to a surface of a glass rod (Fig. 4a). By measuring the cantilever bending just before the detachment, the force was obtained.

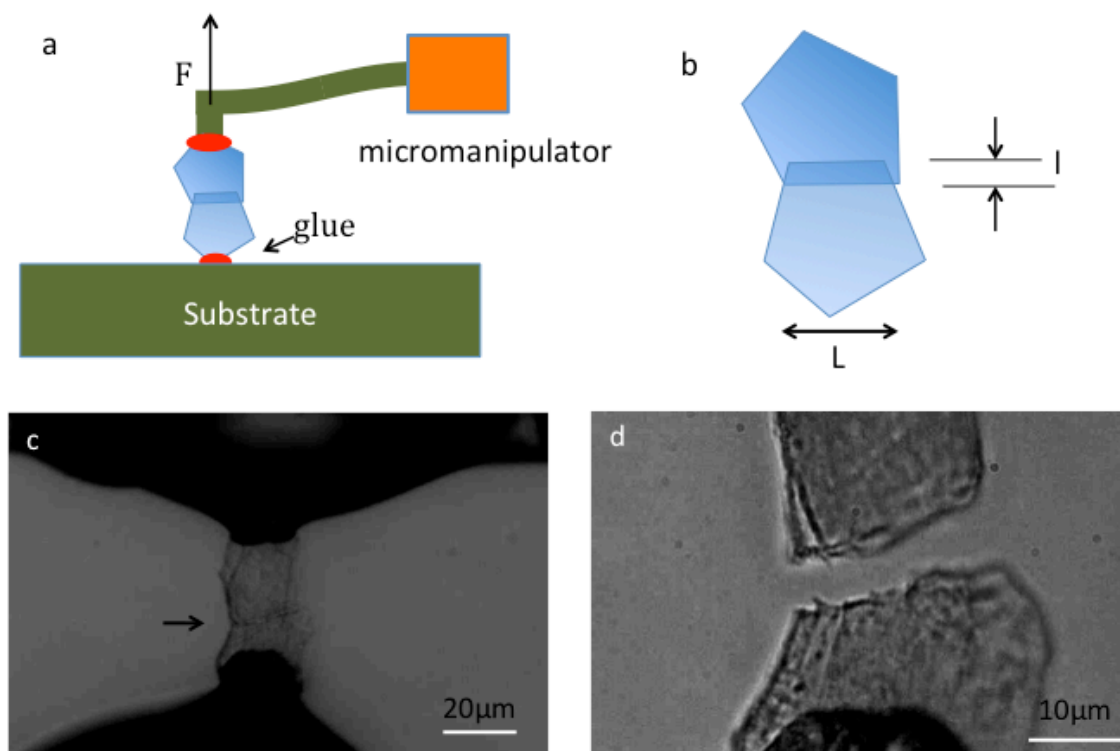


Fig. 4: Measurement of the peripheral separation force of 2 corneocytes. (a) The corneocyte doublet is glued on one side to a glass rod (1mm diameter), and on the other side on a cantilever. (b) The corneocytes have a contact length L and an overlap length l . (c-d) The photos show the doublet before and after detachment.

3. Results:

The corneocyte adhesion was probed at three different depths of the SC : (i) at the stratum disjunctum that corresponds to the outer layer of the SC (1st layer), (ii) below the stratum disjunctum which was made accessible after 4 tape strips of the SC (5th layer), and (iii) at the middle of stratum compactum reached after 9 tape strips of the SC (10th layer).

This was done in two ways: (§3.1) by pulling the corneocytes perpendicularly to their plane and (§3.2) by pulling in the plane of two corneocytes adhering by their edges. Different relative humidities were tested (25%, 44% and 71%). Three batches of SC coming from 3 donors were probed. The variability of the observed adhesion behaviors was large within a batch of SC but statistically similar between two batches (see appendix A). Therefore, the data from the three batches were pooled together.

3.1 Detachment of corneocytes after pulling perpendicularly to the SC:

3.1.1: Normal Stratum Corneum:

When the pulling force was perpendicularly applied by the cantilever to the SC, four different classes of detachments were identified (Fig. 5). The corneocyte detachment

occurred (i) in one step, (ii) in two steps, (iii) leaving the glue partly covered by a corneocyte and partly bare and (iv) the glue did not succeed in detaching any corneocytes. In the outermost layers, there was no spatial correlation between these cases, meaning that two corneocytes located side by side can independently be either strongly or loosely adhering to the SC:

Case I: “One step process”. The pulling force is increased until at some level F_{inter} , the involved corneocyte suddenly detaches from the SC (cf. video at: <https://drive.google.com/file/d/1qdjfwxguJ9cHrtjo12POq39yN-djNACl/view?usp=sharing>). This is an interplanar detachment force F_{inter} (Fig. 6, green crosses).

Case II: “Two-step process”. As the pulling force is increased, the center of a corneocyte becomes first suddenly lifted at a force F_{inter} indicating that some interplanar detachment from the corneocyte immediately below has taken place (Fig. 6, black solid circles), but the corneocyte remains retained through its edges (peripheral adhesion) attached to its neighbors. Then to complete the detachment, a second step is needed, consisting in an increase of the pulling force (not measured) (c.f. video at: https://drive.google.com/file/d/1MWBPUYWiRnffss_qCiCPvif2NjFuF7Sa/view?usp=sharing).

Case III: “Glue partially covered”. After detachment, the glue at the cantilever tip is only partly covered by a corneocyte (Fig. 6, red triangles). This case occurs when the glue is in contact with two corneocytes, one of which detaches easily while the other is not detached by the glue (cf. video at: https://drive.google.com/file/d/1JP37vf_gF36XVIQ9C1y00ipQyVmJgz34/view?usp=sharing). The detachment force is a combination of interplanar corneocyte detachment force F_{inter} and glue/corneocyte detachment force $F_{\text{g-c}}$.

Case IV: “No detachment”. The glue detaches from the corneocyte at the force $F_{\text{g-c}}$ (cf. video at: <https://drive.google.com/file/d/1eSTs3pc4ZxT8RS035NrQig8lEOY9n12l/view?usp=sharing>). This implies that the involved corneocytes are firmly attached to the SC and that their detachment force is larger than $F_{\text{g-c}}$ (Fig. 6, open black circles).

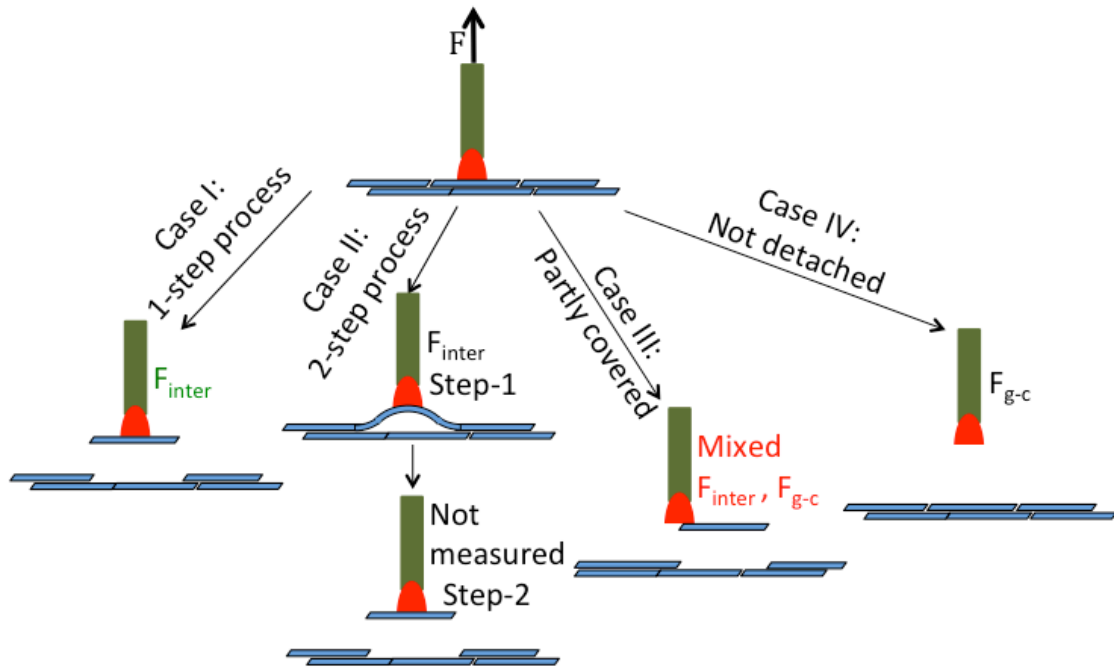


Fig. 5: The 4 cases of detachments when a cantilever pulls on the stratum corneum. Case I (1-step detachment), the pulling force is increased until at some level F_{inter} , the involved corneocyte suddenly detaches entirely from the SC. Case II (2-steps detachment): as the pulling force is increased, the center of a corneocyte becomes first suddenly lifted at a force F_{inter} indicating that some interplanar detachment from the corneocyte immediately below has taken place, this F_{inter} force is measured, but the corneocyte remains retained through its edges (peripheral adhesion) attached to its neighbors. Then to complete the detachment, a second pulling step is needed, consisting in an increase of the pulling force (this force is not measured). Case III (glue partially covered): after detachment at the force F_{inter} , the glue at the cantilever tip is only partly covered by a corneocyte (Fig. 6, red triangles). Case IV (no corneocyte detachment): the glue detaches from the corneocyte at the (measured) force F_{g-c} but no corneocyte has been detached.

The corneocyte detachment forces shown in Fig. 6 have a large dispersion. The pulling experiments done every $200\mu\text{m}$ show no correlation between two adjacent measurements. These results indicate that the corneocyte population is very heterogeneous in adhesion, with forces that can differ by one order of magnitude for corneocytes located side by side. Moreover, in these experiments, the possibility to quantify the adhesion of corneocytes to SC is inherently limited by the finite adhesive strength ($100\mu\text{N}$ to above $1400\mu\text{N}$) of the bond between the corneocytes and the glue. Therefore, we cannot precisely determine the distribution of the adhesion forces of individual corneocytes to the SC as the high-force side of the distribution is always truncated by the glue-corneocyte bond threshold. One pertinent parameter for comparing the corneocytes adhesion at different depths of the SC is the success rate (SR) that is the ratio of the total number of detachments relative to the total number of

pulling experiments. Fig. 6 shows the data of the pulling experiments for the 1st, 5th and 10th layers of the SC, with diameters of glue in the range 10-20 μ m at a relative humidity (RH) of 44 \pm 6%. It displays the detachment forces of the corneocytes F_{inter} for case 1 (green crosses) and for step1 of case II (filled black circles), the detachment forces of the glue F_{g-c} (open circles) of case 4, and the mixed F_{inter} and F_{g-c} of case III (red triangles). The speed at which the pulling was performed, i.e. the loading rate (LR), was not controlled but was measured afterwards. The detachment forces are plotted as a function of LR and they clearly show that the LR has an effect on the

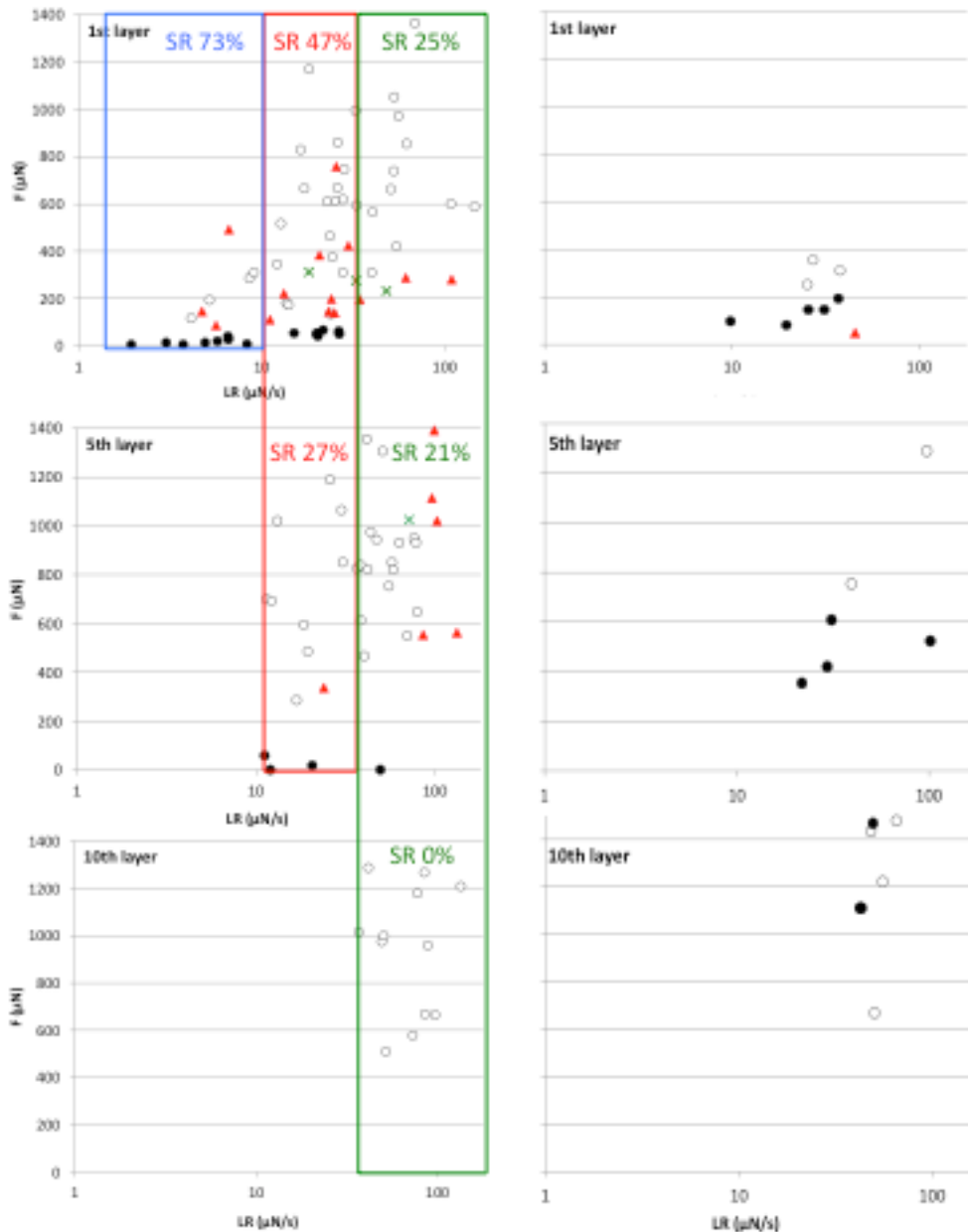


Fig. 6: Corneocyte detachment forces from normal stratum corneum (left side, at RH=44 \pm 6 %) and for SC that has undergone laser micro-dissection (right side, at RH=55 \pm 3%). The forces (Y axis) are plotted versus loading rate (LR) that is the rate at which the pulling force is increased, expressed in microNewtons per second. The force data is plotted as a function of LR (horizontal axis) in order to compare the adhesion for the 1st, 5th, 10th layers for similar ranges of LR because the LR has some effect on the detachment force. The size of glue is between 10 and 20 μ m. The green crosses correspond to the 1-step

detachment forces F_{inter} (case I). The filled black circles correspond to F_{inter} in step 1 of the 2-step detachment forces (case II). The open circles represent F_{g-c} the “no-detachment” cases (case IV). The red triangles represent the detachment forces of glue partially covered cases (case III) that is a mixture of F_{inter} and F_{g-c} . The success rate (SR) indicated in the figure is the ratio of the total number of detachments relative to the total number of pulling experiments. The green rectangle compares the 1st, 5th and 10th layers with the success rate indicated in green for LR in the range 33-180 $\mu\text{N/s}$. The red rectangle compares the 1st and 5th layers at LR values ($10 < LR < 33 \mu\text{N/s}$) for which no data was obtained for the 10th layer; the success rate is indicated in red. The blue rectangle represents the data for the 1st layer with LR below 10 $\mu\text{N/s}$ for which no data was obtained for the 5th layer. The error bars are ± 3 to $\pm 10 \mu\text{N}$ depending on the cantilever stiffness that was used. This corresponds at most to the size of the data points.

layer	LR	Nb tot	Case I	Case II	Case III	Case IV	SR (%)
1st	0-10	15	0	8	3	4	73
	10-33	36	2	7	8	19	47
	33-180	16	1	0	3	12	25
5th	0-10	0					
	10-33	11	0	2	1	8	27
	33-180	24	1	1	3	19	21
10th	0-10	0					
	10-33	0					
	33-180	12	0	0	0	12	0

Table 1: Number of detachments case by case and layer by layer for three loading rates (LR) ranges at RH 44%.

detachment as described further below. Table 1 presents the number of detachments case by case and layer by layer for three LR ranges. To compare the corneocytes adhesion at different depth levels without having the LR-related bias, the detachment forces were compared for the same ranges of LR. The green box includes the data of the three depths for $33 \mu\text{N/s} < LR < 180 \mu\text{N/s}$. These boundaries were chosen to include the maximum number of data points, the most limiting factor being the data points of the 10th layer for which only large values of LR were obtained. They show that the success rate (SR), i.e. the ratio of the number of corneocyte detachments relative to the total number of pulling experiments, decreases upon going from the 1st (25%) to the 5th (21%) and to the 10th layer (0%). Similarly, the red box adds evidence to this variation: the data from the 1st and the 5th layers, for $10 \mu\text{N/s} < LR < 33 \mu\text{N/s}$ shows that the SR decreases from the 1st (47%) to the 5th layer (27%). The SR variation versus LR within the 1st layer shows an effect of LR on the SR (respectively blue and red boxes, 73%, 47%, student test 4.1% with Welch correction). Therefore, the LR has an effect on the detachment forces and on the detachment process, particularly at low LR. As described above, the data shows that corneocytes with an adhesion higher than the glue-corneocyte bond threshold are more frequent in the deeper layers of SC than in the surface layers, and therefore the interplanar adhesion increases in the deeper layers of the SC.

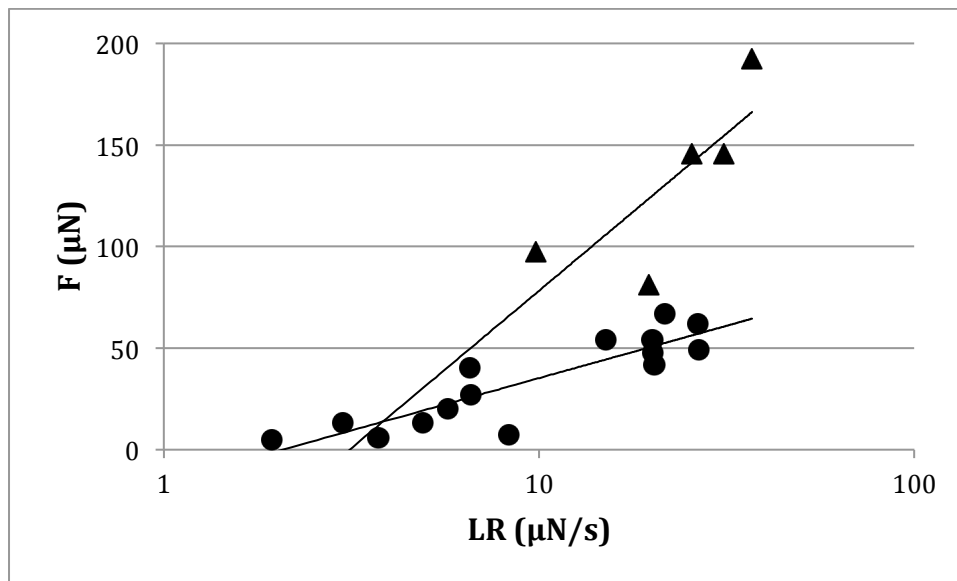


Fig. 7: First step of the 2-step detachment forces versus loading rate in the 1st layer: 1st step detachment forces of corneocytes F_{inter} , for case II versus loading rate (the rate at which the pulling force is increased, expressed in $\mu\text{N/s}$) in the 1st layer, for glue diameters in the range 10-20 μm . The black circles correspond to normal SC, and the black triangles correspond to SC after laser micro-dissection.

The data in Fig. 6 also shows that the case II detachments (black circles) do not occur for LR above 27 $\mu\text{N/s}$. The corresponding data points of Fig. 6 are also reported in Fig. 7 but with a magnified scale. They reveal that the detachment force of the 1st step of case II increases linearly with the $\log(\text{LR})$.

3.1.2 Stratum corneum after Laser micro-dissection:

It may be useful to know if by removing the peripheral links between one corneocyte and its neighbors of the same layer, one could more easily detach the corneocytes. For this purpose, laser micro-dissection (LMD) was used to make a superficial cut on a chosen contour on the SC (20) of the size of one corneocyte and a pulling force was applied at the center of the cut. By cutting superficially a circle at a random position on SC, laser micro-dissection (LMD) offers the opportunity to remove the links between corneocytes inside the circle and its surrounding neighbors of the same layer, leaving only the interplanar links on the corneocyte to be detached from the underlying layers of the SC.

The pulling experiments on SC after LMD were done at an RH of $55 \pm 3\%$. Upon pulling on the corneocyte, the detachment proceeded in the same way as without LMD (video at: https://drive.google.com/file/d/1xplHXutfY5Z_8x7XwUOnYUEa05yxSBD/view?usp=sharing). The success rate (SR) and comparison with the no-LMD experiments are shown in table 2. The SR for LMD experiments is more than twice that of the no-LMD experiments (Fig. 6 and table 2). This suggests that when a large mechanical weakness is generated by a laser micro-dissection around the spot at which the pulling force is applied, the detachment is facilitated (Fig. 6). This is consistent with the fact that higher F_{inter} values are measured with LMD. Indeed, because of the mechanical weakness introduced by LMD and also because of the elimination of the bonds between the corneocyte and its neighbors of the same layer, LMD allowed the detachment of

corneocytes, particularly in the 10th layers which could not be detached with glass microcantilevers before LMD.

The overall behavior with LMD (Fig. 6 right side) is consistent with the one without LMD (Fig. 6 left side), with an interplanar adhesion increasing with depth in the SC, and with the 1st step of case II detachments forces that increase with log(LR) (see fig. 7). However, the low force detachments observed without LMD (step 1 of case II, Fig. 6 left) were not anymore observed with LMD. A likely reason is that the heat due to the laser cutting process generates a strong convection that detaches and removes parts of weakly adhered corneocytes (20). Interestingly, in some cases, fragments of corneocytes were seen flying off during the cutting.

To check that the heat generated by LMD does not destroy the corneodesmosomes at some distance from the cut, controls were made by pulling outside the micro-dissected circles at a distance of 10 μ m (Fig. 3c), at the level of the 5th layer. Table 2 shows the comparison of the controls with the no-LMD cases for LR in the 33-180 μ N/s range. One does not see a dramatic destruction of corneodesmosomes, although this conclusion should be taken with caution because the statistics are weak, given the small number of points (5 points). It is worth noting that a small mechanical weakness created only on one side of the pulling point (as in the controls) does not facilitate the detachment.

layer	LR	No LMD		LMD		LMD controls	
		Nb tot	SR (%)	Nb tot	SR (%)	Nb tot	SR (%)
1st	0-10	15	73	0			
	10-33	36	47	6	67		
	33-180	17	29	3	67		
5th	0-10	0		0		1	100
	10-33	11	27	3	100	0	
	33-180	27	30	3	33	5	20
10th	33-180	12	0	7	43	0	

Table 2: Debonding success rates: comparison between the no-LMD and LMD experiments, and with LMD controls. Here, as the number of LMD data points was too small, the range of the glue droplet size used for comparison of no-LMD/LMD was increased to 10-23 μ m in order to include more points.

3.2 Detachment of corneocytes after pulling in the plane of a corneocyte doublet:

The peripheral adhesion was measured directly on corneocyte doublets (see materials and methods) that were sometimes obtained when pulling perpendicularly to the SC. The forces, which are displayed in Fig. 8a for a narrow range of loading rate (LR), clearly showed an increase of the peripheral adhesion in the deeper layers in the SC. The success rate of separation was 100% in this configuration. It is worth noting that adjacent corneocytes of the same layer have an average overlap length of 3.5 μ m (see Fig. 4). The contact length L of these doublets and their overlap length l were measured before separation.

This peripheral adhesion (i.e. the adhesion of corneocytes by their edges) could also be characterized in another way, from the perpendicular pulling experiments: after the interplanar separation is achieved (step 1 of case II) and when the pulling force is

increased, the corneocyte is under an increasing tension τ until it detaches (step 2 of case II) from its adjacent peripheral neighbors; to access the tension at which the detachment will occur, one needs a relation between τ and the applied force F (of step 2 case II); this force is equal to the projection of τ on the axis of F , multiplied by the corneocyte perimeter P . The calculation of τ requires the knowledge of the angle θ between the lifted corneocyte and the stratum corneum: $\tau = \frac{F}{\sin\theta \times P}$. This angle was theoretically predicted and it is close to $\pi/4$. Its calculation is given in the appendix B. The values of τ at detachment, expressed in N/m units are presented in Fig. 8b and labeled "indirect". The force data measured directly on doublets (Fig. 8a) divided by the contact length is the tension at detachment, and is also presented in Fig. 8b and labeled "direct". Both methods show a clear increase of the detachment force with depth.

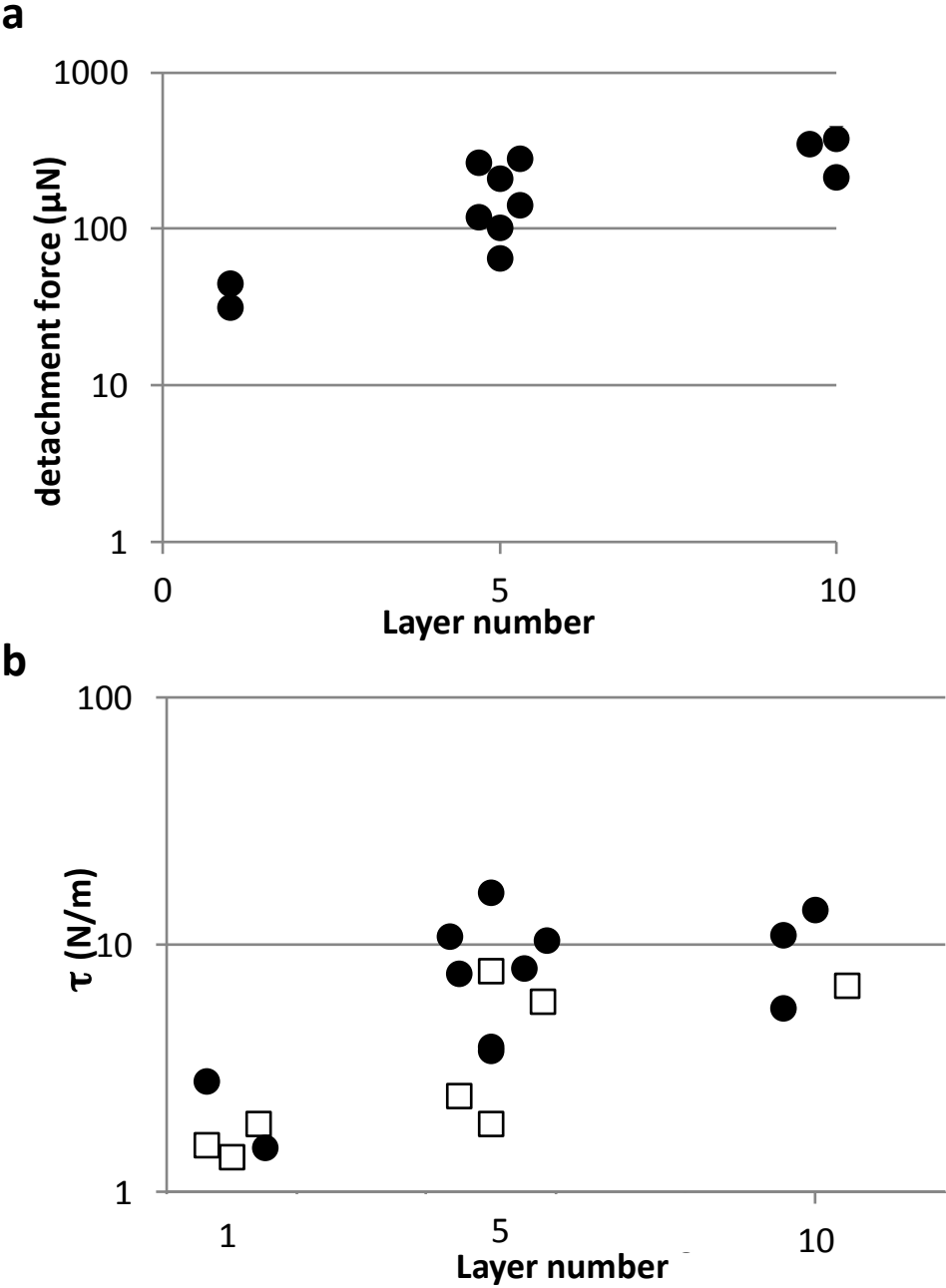


Fig. 8: Measurements of corneocytes peripheral adhesion as a function of the depth characterized by the layer number in the stratum corneum (SC) for $10 < LR < 30 \mu\text{N/s}$. LR is the loading rate, i.e. the speed of pulling. (a) detachment force measured directly (cf. Fig. 4). (b) Detachment tension τ as a function of the layer number. Solid circles represent the force from direct measurements divided by the length of the contact of two corneocytes. Open squares represent the detachment tension τ data obtained indirectly from the perpendicular pulling force F of step 2-case II by using the equation : $\tau = \frac{F}{\sin\theta \times P}$ where P is the corneocyte perimeter and θ is the angle between the lifted corneocyte and the stratum corneum (see fig. B of appendix B).

3.3 Effect of relative humidity (RH):

While the above measurements were performed at 44% RH (except for LMD studies which were performed at 55%RH), the corneocyte adhesion properties were also explored at 71% and 25% RH. Fig. 9 reports the data obtained for these three RH with LR in the range 20-60 in $\mu\text{N/s}$. Raising the relative humidity to 71% increased the success rate from 47% (at 44% RH) to 60% in similar conditions of LR and size of the glue droplet (Fig. 9). In contrast, lowering the RH to 25% decreased the success rate of detachment from 47% to 5%, i.e. almost a factor of 10. The student test (with Welch correction) between 44% and 25%RH gives 0.0003% is a proof that the effect of RH on the adhesion was established. For the 1st layer, this means that for over 20 pulling experiments, only one successful detachment was obtained. Therefore, the detachment force of corneocytes is much higher at very low RH than at 44% RH. Increasing the RH from 44% to 71% did not change appreciably the peripheral detachment forces per unit length ($8.8 \pm 3.8 \text{N/m}$ at 44% RH and $6.7 \pm 3.4 \text{N/m}$ at 71% RH, 8 measurements for each RH level) suggesting that the adhesion is practically unchanged.

This increase of the detachment forces under dry (25%RH) conditions may result from two factors. First, it is known that the Young's modulus (stiffness) of the corneocytes is extremely sensitive to humidity. The dependence of the detachment force on the RH suggests that the mechanical deformation may contribute significantly to the adhesive failure via peeling-type detachment (21). Second, in dry skin samples, the corneocytes have been observed to have rough edges that can produce a « mechanical lock » effect due to interdigitation of adjacent corneocytes at their edges (22) and may add resistance to separation.

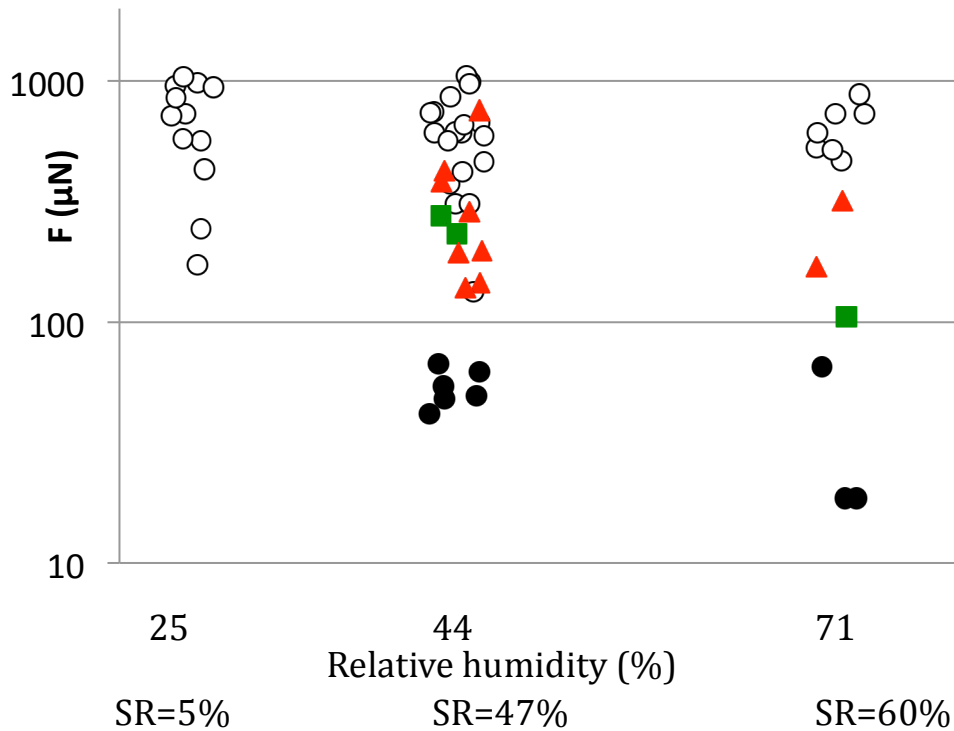


Fig. 9 : Effect of relative humidity (RH) on the interplanar detachment forces of the 1st layer. Values of the detachment forces at $25\pm 4\%$, $44\pm 6\%$ and $71\pm 4\%$ RH. The loading rate (LR), i.e. the speed of pulling, was between 20 and $60\mu\text{N/s}$, and the size of the glue between 10 and $20\mu\text{m}$. The forces F_{inter} for case 1 are displayed as green squares; forces corresponding to step1 of case II are displayed as filled black circles; the detachment forces of the glue F_{g-c} are the open circles (case 4); the mixed F_{inter} and F_{g-c} of case III (glue partially covered) are displayed as red triangles. The student test (with Welch correction) between the success rates (SR) at 44% and at 25% RH gives 0.0003% .

4. Discussion

The dependence of the corneocyte detachment forces with LR deserves comments. The effect of loading rate on separation forces is well documented. Ghattak et al. (23) give many interesting ideas on the relationship between the interfacial dissipation, the length of the interfacial bridges and the crack propagation. They address the issue of the relation between the speed of crack propagation and the fracture energy by using the kinetic theory of bond rupture. Similarly, it is of interest to invoke this theory to explain the present data in which the adhesion at the corneocyte/SC interface mainly stems from bonds between corneodesmosomes (CDs) while the glue/corneocyte interface involves other types of bonds. The dependence of the detachment force on LR is consistent with a transition through different activation barriers. When an increasing pulling force is applied to the glue, a parallel loading is exerted on all these bonds at the glue/corneocyte and corneocyte/SC interfaces. Some bonds will break and induce local detachments of the surfaces. The level of force at which these bonds break is related to energy barriers following Arrhenius law even if the temperature is kept constant because increasing the temperature or allowing time for large thermal fluctuations to break the bonds is equivalent. After each bond rupture, the pulling force is redistributed over the remaining bonds. Bonds keep breaking until the force per remaining bond

reaches a value close to the most probable rupture force (24) inducing the abrupt rupture of all the bonds. This occurs both at the glue/corneocyte and corneocyte/SC interfaces, and the total separation takes place at the weakest interface. At a given load at low LR, a number of bonds spontaneously break because enough time is left for thermal fluctuations to break them; the force for total detachment is proportional to the number of remaining bonds and to the most probable rupture force. At the same load but at higher LR, less bonds have been broken; there are therefore more bonds and the most probable rupture force is higher, leading to a higher separation force. This explains the increase of the detachment force F_{inter} with LR.

The data of Fig. 6 shows an increase of the adhesion with depth in SC. To characterize further the adhesion of corneocytes in SC, there is also an interest to compare their peripheral adhesion with their interplanar one. A reliable parameter to describe adhesion is the adhesion energy. The notion of adhesive force capacity (25) is also interesting because it relates the pull off force with the adhesive and dissipation processes involved in detachments. However, in the present experiments, subtle effects involving the interplay of energy dissipation, elasticity and force dynamic spectroscopy make the analysis complex. One could alternatively describe the adhesion empirically by using the pulling pressure, i.e. the detachment force divided by the area over which the force is transmitted. Because corneocytes are flexible objects, the latter area is not the whole surface of the corneocyte but it is the area of contact with the glue. Indeed, when the corneocyte is under the pulling force transmitted by the glue, the corneocyte deforms and therefore only the region of the cell in contact with the glue is lifted (by approximately the size of the adhesion proteins, $\sim 0.02\mu\text{m}$). The calculation of pulling pressures is done in the next paragraph.

4.1 Comparison of interplanar with peripheral adhesion

In the 1-step process (§3.1.1, case I), the detachments from the underneath corneocytes and from the neighboring corneocytes in the same layer take place continuously. This suggests that the magnitude of the interplanar and peripheral adhesions are very similar (video at: <https://drive.google.com/file/d/1qdfwxguJ9cHrtjo12POq39yN-djNACl/view?usp=sharing>). Three case I events were obtained with $20 < LR < 50 \mu\text{N/s}$ for the 1st layer; they give an average pulling pressure of 1.6 ± 0.6 MPa for the interplanar and the peripheral adhesions of these corneocytes.

The 2-step detachment process (case II) is quite different: the corneocyte becomes firstly detached from the underneath corneocytes in the layer below but the process stops at its edge with its neighbors of the same layer (peripheral adhesion), thus requiring an increased force to complete the detachment (video at: https://drive.google.com/file/d/1MWBPUYWiRnffss_qCiCPvif2NjFuF7Sa/view?usp=sharing). This indicates that these corneocytes have a peripheral adhesion stronger than their interplanar one. Similarly as case I, the detachment pulling pressure was calculated: for the 1st layer, averaged over the 6 values for case II interplanar detachments with $20 < LR < 30 \mu\text{N/s}$, the detachment pulling pressure was 0.44 ± 0.1 MPa which is 4 times smaller than the measure of 1.6 MPa for case I. This suggests an estimate of the ratio of peripheral to interplanar adhesion of 4 for these corneocytes. In addition, this two-step detachment process is more frequently found than the one-step

(case I): in the 1st layer, over 62 pulling experiments, 15 case II and 3 case I detachments were obtained, and the 5th layer showed a similar behavior. It can be concluded that in the most superficial layers of SC, the majority of detached cells have a weaker interplanar adhesion than peripheral.

4.2 Anisotropic adhesion and protective barrier role of SC:

The increase of the delamination energy which is similar to the interplanar adhesion with depth in SC has been already reported for corneocyte layers (14,15) but not for single corneocytes. The present data shows that this is also observed at the level of single corneocytes. Moreover, it is demonstrated here for the first time that the peripheral adhesion similarly increased in the deeper layers of SC (Fig. 8). The increasing adhesion of corneocytes for deeper layers ensures a dynamic stability of the SC. It favors the sturdiness of SC in the context of the corneocytes turnover: new corneocytes adhering strongly to each other push the older ones toward the SC surface while the old corneocytes leave the SC by desquamation, a process in which the loss of their adherence allows them to detach from the SC without being subjected to any force.

However, given the high level of stresses that skin undergoes, this adhesion gradient alone does not optimize the protective role of SC. The anisotropy of corneocytes adherence, i.e., a peripheral adherence which is stronger than the interplanar one, can enhance this role. A first explanation of this adhesion heterogeneity can be found in the literature (11,22,26,27): in the corneocytes at the surface of the SC, a large part of the corneodesmosomes of the central area are degraded while the peripheral ones retain their integrity (11). This can also explain the typical “basket weave” appearance of the outer SC layers in the microscopic images of epidermal sections (11). The high peripheral adherence of corneocytes in the SC allows them to form tight layers able to resist strong stresses. Arranged in stacks, they form a very efficient barrier, particularly in the context of desquamation. Had it been otherwise, i.e. a stronger interplanar adherence along with a weaker peripheral adherence, the SC would be more permeable to the outside medium. The slightest stretching of skin would be propitious to the formation of cracks and clefts in the corneodesmosome-depleted regions, especially where they coincide at adjacent layers. Statistically unavoidable, they would weaken the robustness of SC. It is interesting to note that epithelial tissues have protective cells arranged in a similar way, and that some plants too have surface cells with atypical shapes that play a similar role of protection against outside medium (1).

This adhesion anisotropy also plays a crucial role in ensuring that desquamation occurs in a remarkably synchronized manner, layer by layer, over surfaces that are much larger than a single corneocyte. Indeed, SC topology and adhesion anisotropy makes the outer SC layers more “fragile” once the first corneocytes are removed to produce “gaps” in the layer. Then the layer will be disassembled before the next layer becomes fully exposed for desquamation. This is highly important from a physiological point of view, ensuring skin’s smoothness and avoiding irregular desquamation. Conversely, alterations in adhesive patterns within the SC is known to lead to a number of cosmetic and dermatological disorders (e.g., dandruff etc.) (28).

5. Conclusion

The adhesion of single corneocytes was probed at three depths in the SC with the possibility of distinguishing the interplanar from the peripheral adhesion. It was found that both adhesions increase notably with depth. Close to the SC surface, the peripheral adhesion is substantially higher than the interplanar one. At the SC surface, about half of the corneocytes are loosely adherent and these were detached by the glue. The loosely adhering corneocyte fraction decreases dramatically in the deep layers (5th: ~30%; 10th: ~0%). The corneocyte population is very heterogeneous in terms of adhesion, with detachment forces that can differ by an order of magnitude for corneocytes located side by side. The anisotropy of the adhesion is consistent with the protective barrier role of the SC that can sustain severe mechanical stresses. The gradient and anisotropy of the corneocyte's adhesion explain the dynamic stability of SC and how it resists stretching and shearing forces while still being an impenetrable barrier. The cohesion of SC is strongly increased at low relative humidity, suggesting that more efficient adhesion and cell interlocking contributes to the barrier function of the SC. With detachment processes that depend on the loading rate, the modeling of these experiments is quite a challenge and requires descriptions that involve Arrhenius energy barriers and viscoelasticity. Here, the corneocytes are in their native state as they are detached mechanically from SC in air without action of chemicals or excess water, enabling to obtain biologically relevant results. This overall approach used here can be generalized to study the protective role of many biological tissues found in nature such as epithelial tissues, and some plant tissues that share some geometrical features with SC (1).

Acknowledgements: This work has been financed by l'Oréal. The authors thank F. Pincet from LPS-ENS for fruitful discussions, and C. Goncalves and J. Quintas for the construction of the incubator in the microscope setup. Contribution of A. Potter from L'Oréal for motivation and design of the project and for technical assistance of C. Baltenneck from L'Oréal at the early stages of the project are gratefully acknowledged.

References

1. Barthlott W (1981) Epidermal and seed surface characters of plants: systematic applicability and some evolutionary aspects. *Nord. J. Bot.* 1:345-355.

2. Miroshnikova YA, *et al.* (2018) Adhesion forces and cortical tension couple cell proliferation and differentiation to drive epidermal stratification, *Nature Cell Biol.* 20:69-80.
3. Rawlings AV, Scott IR, Harding CR, & Bowser PA (1994) Stratum corneum moisturization at the molecular level. *J Invest Dermatol* 103(5):731-741.
4. Matsui T & Amagai M (2015) Dissecting the formation, structure and barrier function of the stratum corneum. *Int Immunol* 27(6):269-280.
5. Menon GK, Cleary GW, & Lane ME (2012) The structure and function of the stratum corneum. *Int J Pharm* 435(1):3-9.
6. Simon M, *et al.* (2001) Refined characterization of corneodesmosin proteolysis during terminal differentiation of human epidermis and its relationship to desquamation. *J Biol Chem* 276(23):20292-20299.
7. Rankl C, *et al.* (2010) Detection of corneodesmosin on the surface of stratum corneum using atomic force microscopy. *Exp Dermatol* 19(11):1014-1019.
8. Haftek M, *et al.* (1997) Expression of corneodesmosin in the granular layer and stratum corneum of normal and diseased epidermis. *Br J Dermatol* 137(6):864-873.
9. Abdayem R, Formanek F, Minondo AM, Potter A, & Haftek M (2016) Cell surface glycans in the human stratum corneum: distribution and depth-related changes. *Exp Dermatol* 25(11):865-871.
10. Simon M, *et al.* (2001) Persistence of both peripheral and non-peripheral corneodesmosomes in the upper stratum corneum of winter xerosis skin versus only peripheral in normal skin. *J Invest Dermatol* 116(1):23-30.
11. Naoe Y, Hata T, Tanigawa K, Kimura H, & Masunaga T (2010) Bidimensional analysis of desmoglein 1 distribution on the outermost corneocytes provides the structural and functional information of the stratum corneum. *J Dermatol Sci* 57(3):192-198.
12. Alvarez-Asencio R, *et al.* (2016) Nanomechanical properties of human skin and introduction of a novel hair indenter. *J Mech Behav Biomed Mater* 54:185-193.
13. Chapman SJ & Walsh A (1990) Desmosomes, corneosomes and desquamation. An ultrastructural study of adult pig epidermis. *Arch Dermatol Res* 282(5):304-310.
14. Wu KS, Stefik MM, Ananthapadmanabhan KP, & Dauskardt RH (2006) Graded delamination behavior of human stratum corneum. *Biomaterials* 27(34):5861-5870.
15. Levi K, *et al.* (2008) Effect of corneodesmosome degradation on the intercellular delamination of human stratum corneum. *J Invest Dermatol* 128(9):2345-2347.
16. Rawlings AV & Matts PJ (2005) Stratum corneum moisturization at the molecular level: an update in relation to the dry skin cycle. *J Invest Dermatol* 124(6):1099-1110.
17. Rawlings AV (2010) The stratum corneum and ageing. Textbook of ageing skin, ed Farage MAM, K.W.; Maibach, H.I. (Springer-Verlag, Berlin, Heidelberg), pp 56-75.
18. Leveque JL, Poelman MC, de Rigal J, & Kligman AM (1988) Are corneocytes elastic? *Dermatologica* 176(2):65-69.
19. Garson JC, Doucet J, Leveque JL, & Tsoucaris G (1991) Oriented structure in human stratum corneum revealed by X-ray diffraction. *J Invest Dermatol* 96(1):43-49.

20. Vogel A, et al. (2007) Mechanisms of laser-induced dissection and transport of histologic specimens. *Biophys J* 93(12):4481-4500.
21. Peng Z & Chen S (2015) Effect of bending stiffness on the peeling behavior of an elastic thin film on a rigid substrate. *Phys Rev E Stat Nonlin Soft Matter Phys* 91(4):042401.
22. Iwai I, et al. (2012) The human skin barrier is organized as stacked bilayers of fully extended ceramides with cholesterol molecules associated with the ceramide sphingoid moiety. *J Invest Dermatol* 132(9):2215-2225.
23. Ghatak A, Vorvolakos K, She H, Malotky DL, and Chaudhury MK (2000) Interfacial Rate Processes in Adhesion and Friction, *J. Phys. Chem. B*, 104 (17): 4018–4030.
24. Evans E. (1998) Energy landscapes of biomolecular adhesion and receptor anchoring at interfaces explored with dynamic force spectroscopy, *Faraday Discuss.* 111:1.
25. Crosby AJ *et al.* (2013) Scaling Normal Adhesion Force Capacity with a Generalized Parameter *Langmuir* 29:11022-11027
26. Ishida-Yamamoto A, Igawa S, & Kishibe M (2011) Order and disorder in corneocyte adhesion. *J Dermatol* 38(7):645-654.
27. Corcuff P, Fiat F, & Minondo AM (2001) Ultrastructure of the human stratum corneum. *Skin Pharmacol Appl Skin Physiol* 14 Suppl 1:4-9.
28. Potter AL, G.; Santoprete, R., Querleux, B. (2009) Stratum corneum biomechanics. Skin moisturization, ed Rawlings AVL, *J. (Informa healthcare)*, pp 259-278.

Appendices

Appendix A: Comparison between two different batches

With regard to the pooling the data with different batches of SC, most of the data was obtained with one batch (A2186), but a small number of experiments were done with two other batches. As an example, Fig. A1 displays two sets of data obtained with two different batches (A2186 and A2609) with the same loading rate. Although there is a small number of data points for batch A2609 (number 2 in the graph), the overall adhesion behaviors of the two batches are quite similar. We have the same type of data by comparing A2186 with another batch.

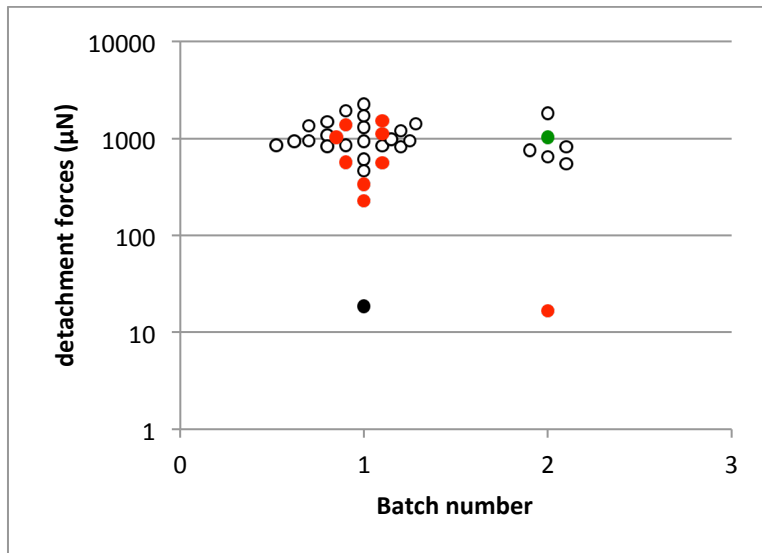


Fig. A1: Comparison of 2 different batches (A2186 and A2609 noted respectively “1” and “2” in the graph) for detachment forces at the 5th layer at high loading rate between. Green, black, red and open circles refer respectively to cases I, II, III and IV. Both batches come from 2 different donors with similar ages.

Appendix B: Obtaining the peripheral detachment force from the total detachment force in the 2-step process

After the interplanar detachment, the corneocyte is retained by the SC only by its peripheral interactions. When the force is increased, the corneocyte further detaches until it completely separates from its neighbors. It is possible to deduce the peripheral separation force from this total detachment force. We have measured it in pulling experiments for each depth (1st, 5th, 10th).

To relate the pulling force to the tension τ of the corneocyte, it is necessary to describe the corneocyte geometry after the interplanar detachment during the increase of the force as shown in Fig. B1.

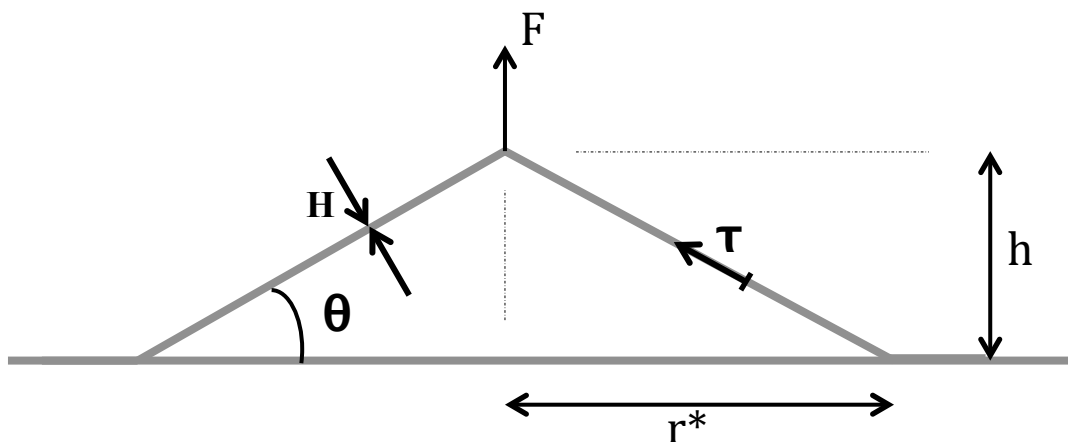


Fig. B1: Geometrical description of corneocytes detachment. The corneocytes (thick grey line) with a thickness H is pulled by a force F applied on one point that rises at the height h .

The tension of the corneocytes is τ , and the corneocyte with part of its neighbors are detached from the SC at an angle θ over a circle of radius r^* .

To deduce τ , one has to obtain an estimation of θ . The relation between the pulling force F and the corneocyte tension τ is :

$$\tau = \frac{F}{\sin\theta \times P}. \quad (\text{B1})$$

where P is the perimeter of the detached corneocyte, accessible from the photos taken after detachment. To derive θ , it is useful to consider an elastic film of thickness H (the thickness of one corneocyte) and of Young's modulus Y adhering on a solid substrate and pulled at one region with the force F . The area over which the force is applied (circle with 15 μm diameter) is approximated as a point. To estimate the different contributions to the energy of the system after an interplanar detachment and before complete detachment, it is reasonable to assume that the corneocyte is detached from the SC by forming a blister with a circular shape of radius r^* and of height h . The corneocyte is bent because it detaches from its initial plane. It is stretched because of the increase in lengths in the radial direction. The detachment requires energy to overcome the adhesion energy σ . The bending energy is:

$$\mathcal{E}_{bend} \sim Y\pi(r^{*2})H^3 \left(\frac{h^2}{r^{*4}}\right) \sim YH^3 \frac{h^2}{r^{*2}} \quad (\text{B 2})$$

The stretching energy is:

$$\mathcal{E}_{stretch} \sim Y\pi(r^{*2})H\left(\frac{h}{r^*}\right)^4 \sim YH \frac{h^4}{r^{*2}} \quad (\text{B 3})$$

The contribution from the adhesion energy σ is proportional to the area lifted from the substrate:

$$\mathcal{E}_{adhes} = \sigma\pi(r^{*2}) \quad (\text{B 4})$$

The last contribution comes from the work of the force to detach the corneocyte:

$$\mathcal{E}_{trac} = -Fh \quad (\text{B 5})$$

The total energy to be minimized is the sum of the traction energy, the surface energy and the elastic energy. To simplify the calculations, we used dimensionless units. H as a unit length for h , $(YH^5/\sigma)^{1/4}$ is a unit length for r^* , $((\sigma YH^3)^{1/2})$ is a unit for F , and $(\sigma YH^5)^{1/2}$ is a

unit for \mathcal{E} . The total energy becomes:

$$\mathcal{E}_{tot} = -Fh + r^{*2} + \frac{1}{r^{*2}}(h^2 + h^4) \quad (\text{B 6})$$

The values of the parameters were determined by minimizing the total energy relative to h and to r^* . This yields after algebra calculation:

$$r^* = (h^2 + h^4)^{1/4} \quad (\text{B 7})$$

$$\tan\theta = h/r^*$$

$$\tan\theta = h^{1/2}/(1+h^2)^{1/4}$$

for $h > 1$, this function is close to 1, to a good approximation. As H (thickness of one corneocyte $\sim 0.2-0.5\mu\text{m}$) is a unit length for h , and as the interplanar detachment is easily seen in the microscope, h is of the order of a few μm . Therefore, for $h > 1$, $\tan\theta$ is close to 1 and θ is close to $\pi/4$, in agreement with video at:

https://drive.google.com/file/d/1MWBPUYWiRnffss_qCiCPvif2NjFuF7Sa/view?usp=sharing

From eqn. (B1), the values of F/L were indirectly obtained for each layer (each value is averaged over 5 experiments):

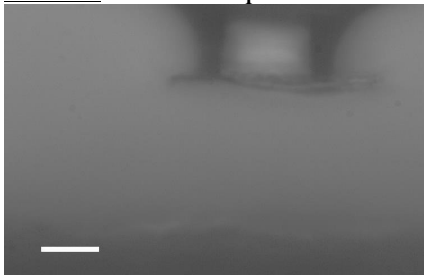
1st: $1.5 \pm 0.3 \text{ N/m}$
5th: $4.5 \pm 1.4 \text{ N/m}$
10th: $13.0 \pm 5 \text{ N/m}$

compared to direct values:

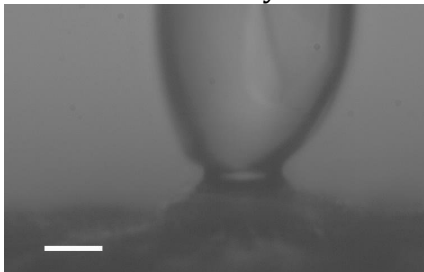
1st: $1.5 \pm 0.7 \text{ N/m}$
5th: $8.8 \pm 1.3 \text{ N/m}$
10th: $13.8 \pm 2.5 \text{ N/m}$

Video captions:

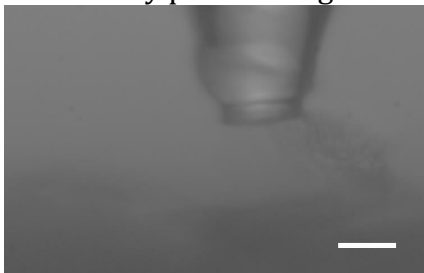
Video1: The 1-step detachment. The scale bar is $10 \mu\text{m}$.



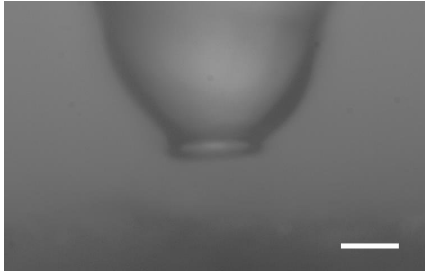
Video2: The 2-step detachment. The first detachment step is clearly visible. Then, the second step is seen. After this, the detached corneocyte is monitored after rotating the cantilever holder by 90° . The scale bar is $10 \mu\text{m}$.



Video3: glue partially covered case; the first detachment of the glue from the corneocyte on the left hand side is easily visible. Then, the second corneocyte becomes progressively detached. After rotating the cantilever holder by 90° , the corneocyte that covers only part of the glue is seen. The scale bar is $10 \mu\text{m}$.



Video4: The corneocyte adhesion is so strong that the glue is unable to detach it from the SC. The scale bar is $10 \mu\text{m}$.



Video5: Detachment after laser microdissection. The scale bar is 10 μ m.

